JOURNAL OF RHEOLOGY

Computer simulation of dilute polymer solutions with the dissipative particle dynamics method

A. G. Schlijper, P. J. Hoogerbrugge, and C. W. Manke

Citation: J. Rheol. **39**, 567 (1995); doi: 10.1122/1.550713
View online: http://dx.doi.org/10.1122/1.550713
View Table of Contents: http://www.journalofrheology.org/resource/1/JORHD2/v39/i3
Published by the The Society of Rheology

Computer simulation of dilute polymer solutions with the dissipative particle dynamics method

A. G. Schlijper

Shell Research Limited, Thornton Research Centre, P.O. Box 1, Chester CH1 3SH, England

P. J. Hoogerbrugge

Shell Research B. V., Koninklijke/Shell Exploratie en Produktie Laboratorium, Postbus 60, 2280 AB Rijswijk, The Netherlands

C. W. Manke[a)]

Wayne State University, Department of Chemical Engineering and Materials Science, Detroit, Michigan 48202

(Received 22 April 1994; accepted 18 January 1995)

Synopsis

A novel method of investigating the link between molecular features of polymer molecules and the rheological properties of dilute polymer solutions has been investigated. It applies the dissipative particle dynamics (DPD) computer simulation technique, which introduces a lattice-gas automata time-stepping procedure into a molecular-dynamics scheme, to model bead-and-spring-type representations of polymer chains. Investigations of static and dynamic scaling relationships show that the scaling of radius of gyration and relaxation time with the number of beads are consistent with the predictions of the Rouse–Zimm model. Both hydrodynamic interaction and excluded volume emerge naturally from the DPD polymer model, indicating that a realistic description of the dynamics of a dilute polymer solution can be obtained within this framework, and that very efficient computer simulations are possible. © *1995 Society of Rheology.*

INTRODUCTION

The rheological properties of dilute solutions of polymers are of interest for a variety of industrial applications; automotive lubrication and oil recovery are two of many. To enable molecular design of polymers targeted at specific applications it is necessary to understand the link between microscopic fluid characteristics (i.e., polymer molecular structure) and macroscopic (i.e., rheological) fluid properties.

The traditional rheological modelling approach to uncovering this link [see Bird *et al.*, (1987)] involves the formulation of a diffusion equation describing the distribution of polymer configurations, from which the configurational averages governing the macroscopic hydrodynamic behavior can be calculated. The diffusion equation is developed from a force balance on "beads" of the polymer chain, in which stochastic forces are

[a)]Corresponding author.

represented by Brownian forces on the beads, and interactions between the polymer and the solvent are usually approximated by a simple bead friction factor. Through these approximations, the solvent is eliminated as an explicit component of the model. Solution of the equations for configurational averages is often very difficult, especially when realistic features of polymer dynamics, such as nonlinear entropic forces, are introduced. Recently, Brownian dynamics simulations [see Zylka and Öttinger (1989)] have been employed to solve the stochastic differential equations governing bead motions numerically, thereby surmounting some of the mathematical difficulties of purely analytical models. Like the diffusion equation approach, however, Brownian dynamics simulations generally do not model solvent motion and polymer–solvent interactions explicitly.

Less traditionally one can, in principle, simulate any fluid model system rigorously at a microscopic level and make the transition to macroscopic variables in large-scale computer simulations (i.e., molecular dynamics simulations). In the case of polymer solutions, however, the time scale separation between the fast solvent relaxation and the slow polymer dynamics makes rigorous molecular-dynamics (MD) simulations a cumbersome, time-consuming, and costly tool. Not until quite recently, thanks to the advent of ultrafast supercomputers, have MD methods been used to investigate relaxation behavior of model polymer chains in solution [Pierleoni and Ryckaert (1992)]. A computationally more efficient way of investigating microscopic behavior and rheological properties of polymer chains in a solvent is offered by the dissipative particle dynamics (DPD) simulation technique as put forward by Hoogerbrugge and Koelman (1992). By introducing a lattice-gas automata time-stepping procedure into the basic MD scheme, they were able to construct a stochastic particle model for an isothermal fluid system that is at the same time computationally much faster than MD and very flexible with respect to the addition of model features. In particular it is easy to introduce bead-and-spring-type polymer chains into the basic fluid, thus obtaining a model for a dilute polymer solution.

The DPD polymer solution model may be regarded as microscopic with respect to the polymer chain, but it is basically a macroscopic model as far as the solvent is concerned (i.e., the solvent is completely characterized in terms of macroscopic parameters such as density and viscosity). However, unlike the bead friction factor representations of hydrodynamic forces employed in traditional bead-spring models, DPD solvent–polymer interactions arise from particle–particle collisions within the simulations. Both polymer and solvent motions propagate consistently from stochastic dynamics at the microscopic scale. Thus the small-scale hydrodynamics of solvent flow, including hydrodynamic interactions among the beads of the polymer chain, are modeled explicitly as a natural consequence of DPD.

Of course, other approaches utilizing more conventional continuum treatments of the solvent might also be employed to obtain similar, explicit representations of solvent hydrodynamics. A numerical solution of the Navier–Stokes equations for the solvent surrounding the polymer beads would be one possible alternative. Simultaneous solution of the Langevin equations for polymer bead motions and stochastic equations governing solvent motion is another possible method. However, the recent success of Koelman and Hoogerbrugge (1993) in modeling concentrated suspension rheology by DPD clearly demonstrates the advantages of the particle-based DPD method in modeling fluids with complex, multibody hydrodynamic interactions. Here we pursue similar computational advantages with our DPD polymer model.

DISSIPATIVE PARTICLE DYNAMICS MODEL

As the polymer model is an obvious extension of the basic fluid model of DPD, we shall briefly describe the basic model first. A more extensive description may be found in

Hoogerbrugge and Koelman (1992). The model consists of N particles moving in a continuum domain of volume V. This domain is effectively replicated in space by means of a standard periodic boundary condition to simulate an infinite medium. As in MD a configuration of the system is specified by all the positions $\mathbf{r_i}$ and momenta $\mathbf{p_i}$. Like lattice-gas automata, the system is updated in discrete time steps δt consisting of a collision phase followed by a propagation phase. In the collision phase momenta are simultaneously updated according to the simple rule

$$\mathbf{p_i}(t+\delta t) = \mathbf{p_i}(t) + \sum_j \Omega_{ij}\mathbf{e_{ij}}, \tag{1}$$

where $\mathbf{e_{ij}}$ is the unit vector pointing from particle j to particle i and the scalar variable Ω specifies the momentum transferred from particle j to particle i. In the propagation phase the particle positions change according to free propagation:

$$\mathbf{r_i}(t+\delta t) = \mathbf{r_i}(t) + \frac{\mathbf{p_i}(t+\delta t)}{m_i}\,\delta t, \tag{2}$$

with m_i being the mass of particle i. In the case at hand, all particles have equal mass m. With an appropriate choice of Ω,

$$\Omega_{ij} = W(|\mathbf{r_i}-\mathbf{r_j}|)[\Pi_0 + \delta\Pi_{ij} - \omega(\mathbf{p_i}-\mathbf{p_j})\cdot\mathbf{e_{ij}}], \tag{3}$$

this setup constitutes a valid fluid-dynamical model, as evidenced by Hoogerbrugge and Koelman (1992). In Eq. (3), $W(r)$ is a dimensionless, non-negative weight function which is zero for $r > r_c$, where r_c is the radius beyond which the particle–particle interaction vanishes. The function $W(r)$ is normalized such that its volume integral is V/N, the inverse of the number density of the particles. The scalar expression between brackets consists of three interaction components, each serving a specific purpose. The first term, Π_0, is a repulsion, which ensures that the particles remain distributed in space homogeneously, and it is directly related to the macroscopic pressure [see Hoogerbrugge and Koelman (1992)]. The second term, $\delta\Pi_{ij}$, is a random number sampled from a (Gaussian or finite-support-homogeneous) distribution with mean zero and variance σ^2; it prevents the formation of crystalline structures and causes fluctuations, i.e., Brownian motion. (Apart from the mean and variance, the exact form of the distribution from which random numbers are drawn has no effect; this is a consequence of the central limit theorem, which says that the results of repeated independent draws from any distribution with a well defined mean and variance will follow a Gaussian distribution.) The third term, containing the dimensionless number ω, is a friction term, which reduces momentum differences without violating overall momentum conservation; it is thus a dissipative term, giving rise to a macroscopic viscosity. Conceptually, the dissipative term models the transfer of energy to modes of motion at length scales less than our mesoscopic point of view, whereas the random (Brownian) term models the transfer the other way.

In the above setup, a natural system of units is defined by m for mass, δt for time, and r_c for length. Consequently and conveniently, we shall take $m = \delta t = r_c = 1$, so that, e.g., the relaxation times that we report below are understood to be multiples of the time step δt. For our simulations, the time step size is held constant at $\delta t = 1$ throughout the calculations. At a value of unity, the DPD time step is effectively self-scaled to the dynamics of the system, producing results that are independent of time step size for the applications studied here. For time step sensitive applications such as temperature studies, the time step size can be varied.

The weight function $W(r)$ introduces a distance dependence into the momentum transfer between two particles. For the work reported here, it was chosen to be $W(r) = 3(1-r)/(\pi n)$, $r < r_c$, with $n = N/V$, the particle number density. Furthermore, $\omega = 4/3$, $\Pi_0 = 1/3$, and $n = 3$; $\delta\Pi_{ij}$ was sampled from a homogeneous distribution on $[-1/3, 1/3]$; hence $\sigma^2 = 1/27$.

Equations (1) and (2) are similar to those of a standard MD simulation, with Ω_{ij} being somewhat analogous to an MD interparticle force. However, the interparticle forces are typically derived from steep potential functions in MD, while the DPD interaction term, given by Eq. (3), is a much "softer" interaction. The computational advantages of DPD relative to MD are achieved because the soft interaction of Eq. (3) allows particle motions on the order of a mean free path during each time step, whereas MD particle motions must be constrained to much smaller distances to accommodate the steep potential functions. Thus the DPD time step can be much larger than the time step in an equivalent MD scheme, while still maintaining accurate solutions of the particle equations of motion.

The important aspect of the DPD algorithm is that it produces a flow of momentum through space that is, to all intents and purposes, identical to that produced by the classical equations of motion that follow from Newton's laws and some reasonable intermolecular potential. The "particles" should not be seen as representations of molecules, but are fairly abstract "carriers of momentum;" perhaps they might be looked upon as akin to the "fluid elements" of classical fluid dynamics: macroscopic with respect to the molecular scale, but small in comparison with gradients of quantities of interest.

Within the framework of this fluid model, a polymer chain can be represented by a linear chain of fluid particles (now called beads) connected by springs: a bead-spring model. In the interaction and propagation phase the polymer beads behave just as the other fluid particles. Besides the ordinary (fluid–fluid) interactions, the polymer beads exchange momentum with their neighbors according to an elastic (spring) force. We chose the Fraenkel spring:

$$\mathbf{F_{ij}} = K(|\mathbf{r_i} - \mathbf{r_j}| - r_{eq})\mathbf{e_{ij}}. \tag{4}$$

Here K is the spring constant and r_{eq} is the equilibrium spring length. Just as the fluid particles may be viewed as packets of fluid, the polymer beads can probably best be viewed as representing polymeric chain segments consisting of a number of monomeric units (Kuhn segments) with some surrounding solvent.

This type of polymer model appears to be very much like the well-known Rouse/Zimm bead-and-spring model, and it can also accommodate various sorts of spring forces to mimic FENE or internal viscosity models [see Bird *et al.* (1987)]. However, the nature of the beads in this model is rather different, since they are assumed to be identical to the fluid particles, to which it is difficult to attach a clear and unambiguous physical interpretation. Therefore simulations with the DPD polymer model have been performed to verify that the essential physical phenomena are reproduced correctly, and to get some feel for the computational effort relative to that of a standard MD simulation for this sort of system. To attain these objectives, radius of gyration, relaxation times, and scaling exponents of the DPD model were obtained and compared to results from traditional Rouse/Zimm models [see Bird *et al.* (1987) and Doi and Edwards (1986)] and to a similar study carried out recently by Pierleoni and Ryckaert (1992) using a standard MD technique. This involved measuring the positional bead autocorrelation function

TABLE I. Results of simulation runs with different model polymers. Units of length and time are arbitrary in this simulation. Note that R_g for the two-bead (dumbbell) model is the root-mean-square average interbead distance; this gives physical meaning to the length scale. Similarly, the time scale can be interpreted in multiples of the corresponding dumbbell relaxation time. This interpretation is irrelevant as far as the scaling is concerned, however.

Periodic box length	Number of particles	Number of beads	Number of time steps (thousands)	R_g	$t1$
			Weak spring results		
5	377	2	419	0.433±.004	63.1±.6
10	3002	2	141	0.433±.007	62.4±.6
5	378	3	206	0.594±.008	132.3±.9
10	3003	3	130	0.584±.013	122
5	379	4	407	0.716±.008	207.6±.6
10	3004	4	402	0.713±.008	210.7±.6
6.41	800	10	1590	1.252±.016	1283.2±1.2
			Strong spring results		
2.17	33	2	1120	0.434±.003	89.5±.3
2.90	76	3	200	0.584±.008	155.4±1.5
4.03	201	5	540	0.812±.011	366.9±.6
6.41	800	10	560	1.247±.028	1305±9
9.25	2394	20	767	1.888±.069	5449±60
12.5	5889	30	1691	2.418±.079	9085±90

$$C(t) = \frac{1}{N}\sum_i \langle[\mathbf{r_i}(t) - \mathbf{R_{cm}}(t)]\cdot[\mathbf{r_i}(0) - \mathbf{R_{cm}}(0)]\rangle, \tag{5}$$

where N is the number of beads in the chain, $\mathbf{r_i}$ denotes the position of bead i, $\mathbf{R_{cm}}$ denotes the position of the center of mass of the chain, and t and 0 denote time. The initial value $C(0)$ is equal to R_g^2, the mean-square radius of gyration, and the time dependence of $C(t)$ contains information on the relaxation spectrum of the polymer in solution. This spectrum, in turn, governs the rheological properties of the fluid in the linear viscoelastic regime.

RESULTS

Two variants of the polymer model have been investigated. The first model is as close an approximation to the classical Rouse/Zimm model as could be obtained within the DPD framework. The spring force was taken as Hookean (i.e., $r_{eq} = 0$) and the spring constant was adjusted such that the average spring length was identical to the average nearest-neighbor distance between solvent particles (which was 0.86). This implied a fairly weak spring ($K = 0.006$); consequently, this model is referred to as the "weak spring" model. The other model employed the Fraenkel spring with an equilibrium length of $r_{eq} = 0.85$ and $K = 0.25$, which results in the same average spring length. This is the "strong spring" model. The autocorrelation function $C(t)$ was measured for chains with a total number of beads ranging from 2 to 30. The radius of gyration was obtained from $C(0)$ and the main relaxation time τ_1 from a fit of log $C(t)$ to the analytical formula for the Rouse/Zimm model (see the Appendix). The simulations were performed in cubic domains (periodic boxes) wherein the box length was increased to accommodate the increase of radius of gyration with bead number, thereby keeping all interactions between

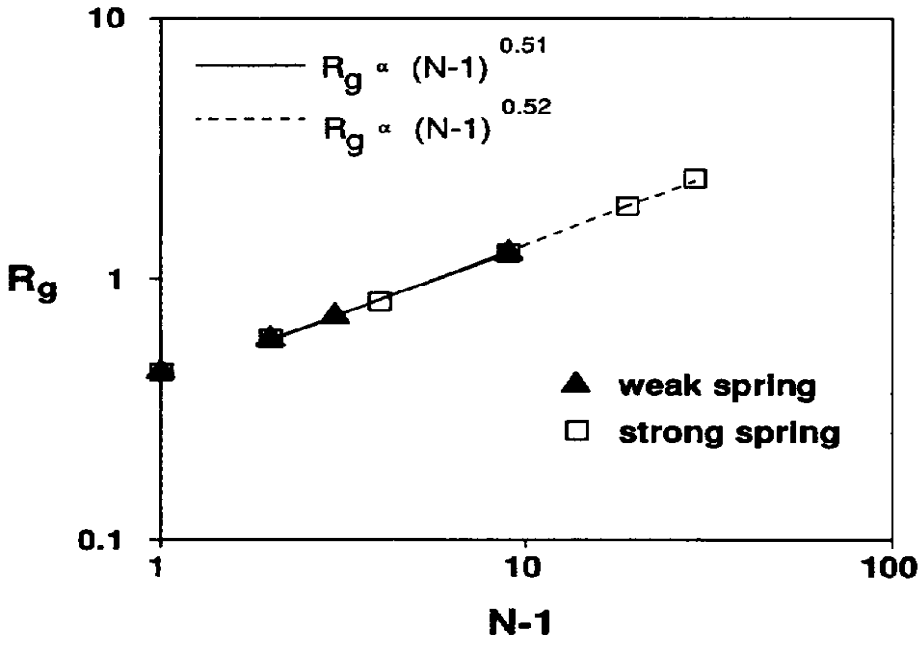

FIG. 1. Scaling of root-mean-square radius of gyration R_g with number of springs $(N-1)$. DPD results for both the weak spring (Hookean spring) and the strong spring (Fraenkel spring) show scaling exponents close to 0.5, the scaling exponent for the Rouse–Zimm model. R_g values are reported in units of r_c, the particle–particle interaction radius.

the polymer chain and image chains in the surrounding periodic boxes small. The relevant data for the various simulation runs and the results are given in Table I.

A scaling analysis of the results (see Figs. 1 and 2) indicates that the radius of gyration varies with the number of springs to approximately the power $\nu = 0.51$ and $\nu = 0.52$ for the weak and strong spring models, respectively. The main relaxation time goes up with the number of beads to the power $\alpha = 1.95$ for the weak spring model and $\alpha = 1.83$ for the strong spring model (see Table II).

These two exponents, α and ν, signal the presence of excluded volume and hydrodynamic interaction, respectively, two aspects of polymer solutions which are difficult to model in a traditional fashion. The best α and ν values for polymers in good solvents are 0.59 and 1.77, respectively [see de Gennes (1979) and references therein]. The simple Rouse model, which neglects both excluded volume and hydrodynamic interaction, predicts $\nu = 0.5$ and $\alpha = 2$. The Zimm model also does not incorporate excluded volume effects, but it does account approximately for hydrodynamic interaction by means of a parameter h^* which can vary between zero (no hydrodynamic interaction at all) and 0.262, a value associated with full hydrodynamic interaction [see Adam and Delsanti (1977)]. With full hydrodynamic interaction the Zimm model predicts $\alpha = 0.5$ and $\nu = 1.5$. Clearly the DPD strong spring model exhibits hydrodynamic interaction and, perhaps to some degree, excluded volume. The weak spring model follows the Rouse model in that it does not seem to exhibit either of these effects. This may be due to the fact that the nearest-neighbor bead distance fluctuates more for the weak spring case, so that beads spend on average more time at a greater separation, which can be expected to delay the onset of the scaling regime to larger values of N. From the fit of log $C(t)$ to the Rouse/Zimm formula, values for the parameter h^* ranging from 0.06 to 0.22 were obtained also; the values are realistic in the sense that, if experimental data are analyzed with a Zimm model, similar values are obtained [see Adam and Delsanti (1977)].

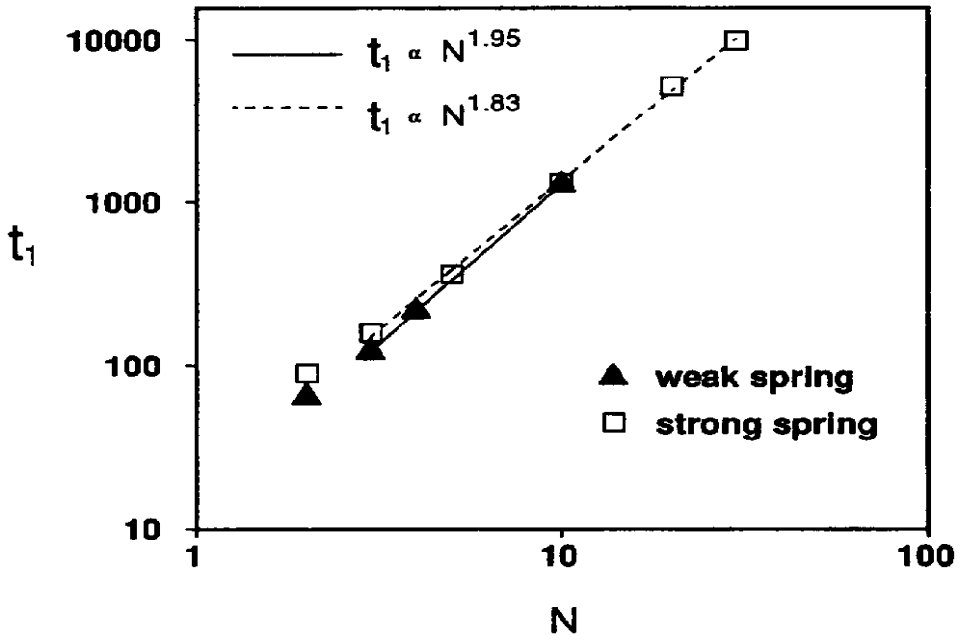

FIG. 2. Scaling of first relaxation time with number of beads. The DPD results for the weak spring (Hookean spring) are close to the scaling exponent of 2.0 for the Rouse model (no hydrodynamic interaction), while the DPD strong spring (Fraenkel spring) scales with N to the 1.8 power, indicating the presence of hydrodynamic interaction (Zimm model). Relaxation times are reported in units of δt, the simulation time step size.

The same scaling exponents α and ν arise in the structure factor $S(q)$ and the intermediate scattering function $S(q,t)$ in the range $qR_g \gg 1$, where the internal structure and motions of the chain are probed. $S(q)$ and $S(q,t)$ can be obtained in a simulation through use of the formulas

$$S(q) = \frac{1}{N}\left\langle \left| \sum_{j=1}^{N} \exp(iqr_j) \right|^2 \right\rangle \tag{6}$$

and

$$S(q,t) = \frac{1}{N}\left\langle \sum_{j=1}^{N}\sum_{k=1}^{N} \exp\{iq[r_j(t)-r_k(0)]\} \right\rangle. \tag{7}$$

TABLE II. Scaling laws for radius of gyration R_g and main relaxation time τ_1: $R_g = (N-1)^{\nu}$ and $\tau_1 = N^{\alpha}$, where N is the number of beads. The difference in ν between the weak and strong spring models is significant if the data on the radius of gyration are accurate to within 3%. The difference in α between the weak and strong spring models is significant if the data on the relaxation time are accurate to within 7%.

Model/experiment	ν	α
Rouse	0.5	2.0
Zimm	0.5	1.5
Experimental (good solvent)	0.59	1.77[a]
DPD weak spring model	0.51±0.01	1.952±0.003
DPD strong spring model	0.52±0.01	1.831±0.004

[a]Not measured directly, but determined from the scaling result $\alpha = 3\nu$.

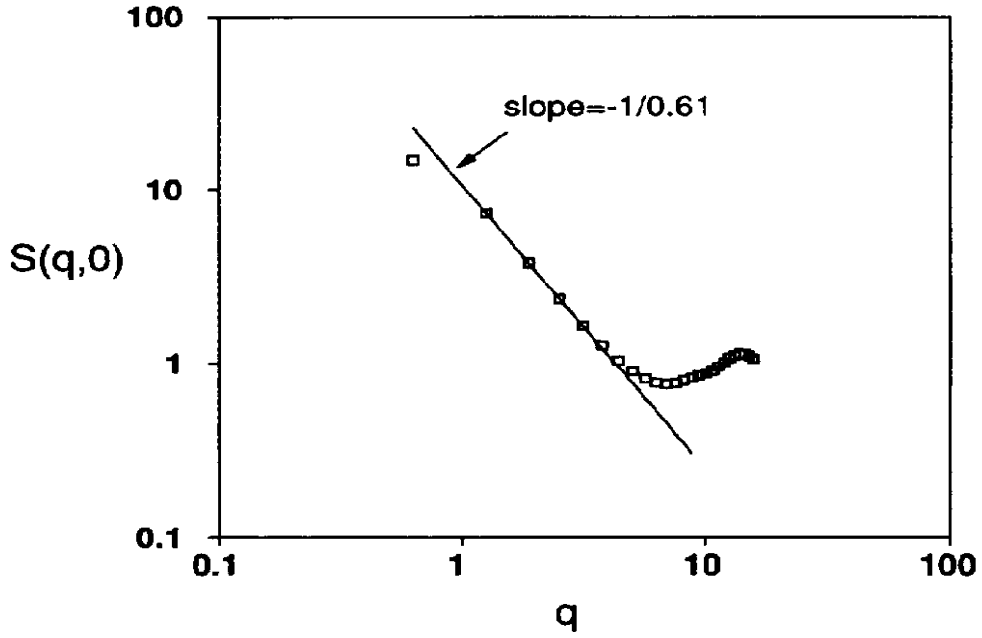

FIG. 3. Structure factor $S(q)$ for simulated 20 bead chain with "strong" (Fraenkel) spring connectors. The slope of the curve at small q values implies a value of 0.61 for the static scaling exponent ν, a value associated with excluded volume chains (good solvents).

The scaling behavior of these functions is

$$S(q) \propto q^{-1/\nu}, \quad S(q,t) = S(q,0)F(q^{\alpha/\nu}t), \tag{8}$$

where F is a universal function for arbitrary wave vector q (note $S(q,0) = S(q)$ and $S(0) = N$). We did a separate simulation with the 20 bead system to record the scattering function at various values of q. For this, we used vectors along the three coordinate directions with magnitudes $2\pi k/L$, $k = 0,1,2,...$, which fits in with the periodic boundary conditions. We calculated only the real part of $S(q,t)$; the imaginary part is zero except for statistical noise. Figure 3 shows $S(q)$ and the slope in the relevant region of the log–log plot. It implies $\nu = 0.61$, in reasonable agreement with the theoretical prediction of 0.59, thus providing stronger evidence of excluded volume than the scaling exponent $\nu = 0.52$ obtained from the R_g measurements for the strong spring. Figure 4 shows $S(q,t)$ vs q^x, where $x \equiv \alpha/\nu$, for various q; the value of $x = 2.7$ yields the best fit. Scaling theory [see de Gennes (1979)] predicts $\alpha/\nu = 3$ in three dimensions. Molecular-dynamics simulations [$x = 2.9 \pm 0.1$; Pierleoni and Ryckaert (1991)] as well as experiments [$x = 2.85 \pm 0.05$; Adam and Delsanti (1977)] yield lower values for x than theory, as we have found for the DPD simulations. Since the N values were relatively small in our DPD simulations, the discrepancy should probably also be attributed to the fact that the true dynamic scaling regime has not been reached yet. The scaling behavior of the Rouse–Zimm model, discussed in the Appendix, suggests that the high-N scaling regime is reached for chains longer than about ten beads.

CONCLUSIONS

From this study we conclude that the DPD polymer model appears to be capable of exhibiting the relaxation and scaling behavior that is characteristic of real polymer solutions, even with a quite small number of beads, and that the two essential phenomena of excluded volume effect and hydrodynamic interaction are evident. The degree to which

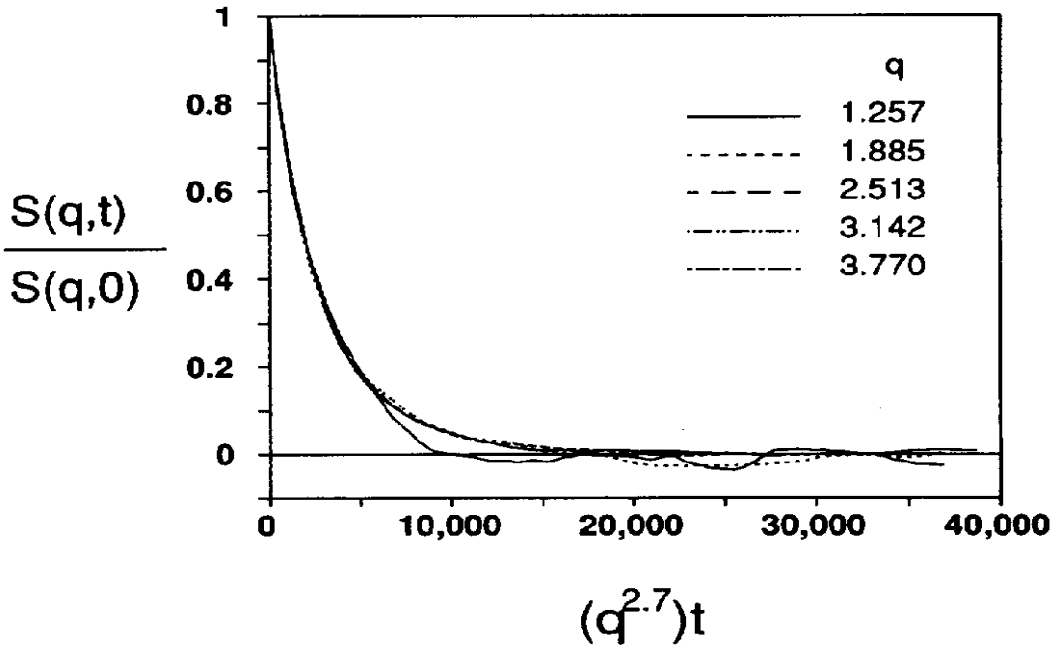

FIG. 4. Scattering function $S(q,t)$ plotted as a function of scaled time for the 20 bead chain with strong (Fraenkel) spring connectors at various values of q. Approximate coalescence to a master curve is produced for the case shown, where t is scaled by $q^{2.7}$.

they are present in the model can be controlled by altering the polymer–solvent interaction and the details of the spring forces that connect the beads of the polymer chain. A detailed quantification of these effects is outside the scope of this investigation and would require additional results for longer polymeric chains.

In comparison with standard MD, the DPD simulation technique has proven to be very quick and inexpensive. The entire set of simulations was performed in the space of two weeks on a Silicon Graphics Crimson workstation, whereas Pierleoni and Ryckaert (1992) report the use of 100 h of CPU time on a Cray XMP to obtain what would seem to be similar results from MD runs. A more quantitative comparison with the work of Pierleoni and Ryckaert can be done by examining the autocorrelation function decay curves and expressing physical times in numbers of time steps; this approach shows that the DPD time step is about 60× as large as an MD time step. Since the computational effort per time step is about the same in both DPD and MD, this comparison suggests that the DPD simulations are about 60× faster than equivalent MD simulations.

APPENDIX A: DECAY OF THE AUTOCORRELATION FUNCTION, AS PREDICTED BY THE ROUSE—ZIMM THEORY

Using Eqs. (11.6-4)–(11.6-7) of Bird *et al.* (1987), the autocorrelation function defined by our Eq. (5) can be written as

$$C(t) = \frac{1}{N} \sum_{i=1}^{N-1} \sum_{j=1}^{N-1} C_{ij} \langle \mathbf{Q_i}(\mathbf{t}) \cdot \mathbf{Q_j}(\mathbf{0}) \rangle, \tag{A1}$$

where the C_{ij} are elements of the Kramers matrix, and $\mathbf{Q_i}$ denotes the vector connecting bead i to bead $i+1$. The vectors $\mathbf{Q_i}$ in Eq. (A1) are then transformed to normal coordi-

nates $\mathbf{Q}_\mathbf{j}'$ by $\mathbf{Q}_\mathbf{i} = \Sigma_{j=1}^{N-1} \Omega_{ij} \mathbf{Q}_\mathbf{j}'$, where $\Omega_{ij} = (2/N)^{1/2} \sin(ij\pi/N)$. [Our notation and mathematical developments follow Chap. 15 of Bird *et al.* (1987).] In the normal coordinate system, $C(t)$ is given by

$$C(t) = \frac{1}{N} \sum_k \sum_l \sum_i \sum_j C_{kl} \Omega_{ki} \Omega_{lj} \langle \mathbf{Q}_\mathbf{i}'(\mathbf{t}) \cdot \mathbf{Q}_\mathbf{j}'(\mathbf{0}) \rangle. \tag{A2}$$

Since the $\mathbf{Q}_\mathbf{i}'$ are independent for a chain at rest, only the terms $\langle \mathbf{Q}_\mathbf{i}'(\mathbf{t}) \cdot \mathbf{Q}_\mathbf{i}'(\mathbf{0}) \rangle$ are correlated, and therefore nonvanishing. Thus Eq. (A2) reduces to

$$C(t) = 1/N \sum_i (1/a_i) \langle \mathbf{Q}_\mathbf{i}'(\mathbf{t}) \cdot \mathbf{Q}_\mathbf{i}'(\mathbf{0}) \rangle, \tag{A3}$$

where the $a_i = 4 \sin^2(i\pi/2N)$ are the eigenvalues of the Rouse matrix. Doi and Edwards (1986) have shown that the Langevin equations for the normal modes of the Rouse model yield time correlation functions that decay as

$$\langle \mathbf{Q}_\mathbf{i}'(\mathbf{t}) \cdot \mathbf{Q}_\mathbf{i}'(\mathbf{0}) \rangle = \langle Q_i'(0)^2 \rangle \exp(-t/\tau_i), \tag{A4}$$

where the τ_i are the Rouse relaxation times. Using Eq. (A4) and the relationship $\Sigma_i (1/a_i) = (N^2 - 1)/6$ [see Bird *et al.* (1987), p. 24] we obtain

$$\frac{C(t)}{\langle R_g^2 \rangle} = \frac{6}{N^2 - 1} \sum_i (1/a_i) \exp\left(-\frac{t}{\tau_i}\right), \tag{A5}$$

where the τ_i are related to τ_1, the largest Rouse relaxation time, by $\tau_i = (a_1/a_i)\tau_1$.

Subject to certain approximations, the Langevin equations for the normal modes of the Zimm model reduce to the same structure as those of the Rouse model [see Doi and Edwards (1986)], yielding time correlation functions that decay according to Eq. (A4) where the τ_i are now the *Zimm* relaxation times. Thus Eq. (A5) can also be used for the case where interbead hydrodynamic interaction is present by employing the Zimm relaxation spectrum $\tau_i = (\tilde{a}_1/\tilde{a}_i)\tau_1$. Hydrodynamic interaction effects are manifested in the Zimm eigenvalues $\tilde{a}_i$. To facilitate computations, we have used the approximate formulas of Thurston (1974) to evaluate the $\tilde{a}_i$ as functions of the hydrodynamic interaction parameter h^*:

$$\tilde{a}_i = a_i \beta (i/N)^\sigma, \tag{A6}$$

$$\beta = 1 - 1.66 h^{*0.78}, \tag{A7}$$

$$\sigma = -1.40 h^{*0.78}. \tag{A8}$$

Relaxation times were evaluated from our simulation data by fitting Eq. (A5) to values of $C(t)/\langle R_g^2 \rangle$ from the simulations, wherein τ_1 and h^* were determined as optimized parameters. A typical fit, shown in Fig. 5, displays excellent agreement between the simulation data and Eq. (A5).

Since Eq. (A5) is rigorous only for the Rouse–Zimm model, it may initially seem surprising that our strong spring simulations, which clearly depart from the Rouse–Zimm spring connector, follow the Rouse–Zimm autocorrelation function decay curve so closely. However, previous studies of linear viscoelastic properties of freely jointed chains of rigid links [see Fixman and Kovac (1974)] and internal viscosity connectors [see Manke and Williams (1993)] provide evidence that the dynamics of freely jointed

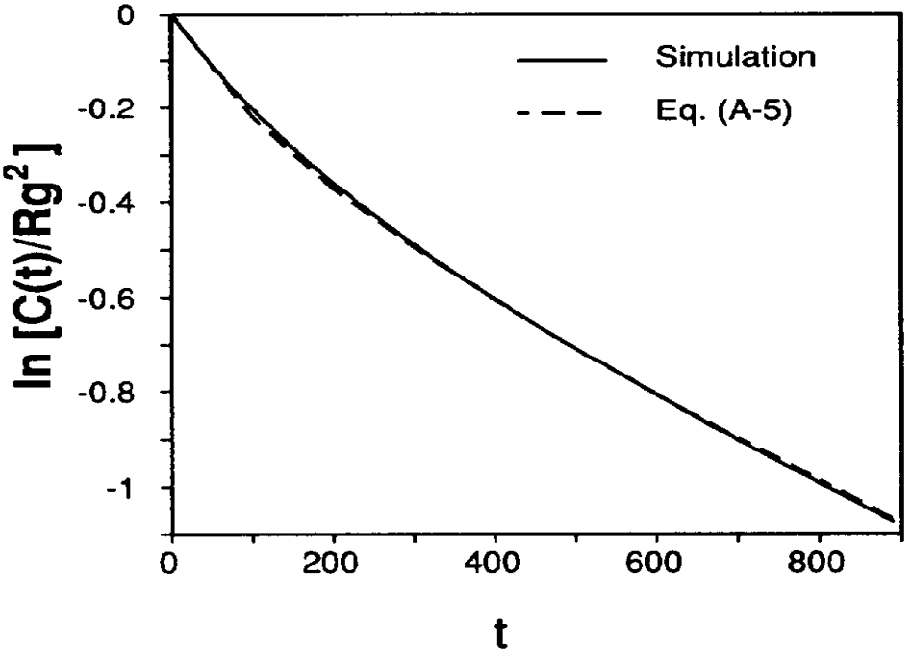

FIG. 5. The decay of the autocorrelation function with time for a DPD simulation of a ten bead chain with strong (Fraenkel) spring connectors is compared with the decay curve predicted by the Zimm model, Eq. (A5). Time t is reported in units of the simulation step size δt.

chains of non-Gaussian connectors follow the Rouse–Zimm relaxation-time spectrum closely under near-equilibrium conditions such as those of the present simulations.

Finally, we have observed that the fitting procedure described above is relatively insensitive to h^*. While the values of h^* obtained from the fitting procedure are plausible, we feel that a much more reliable evaluation of hydrodynamic interaction effects in the DPD simulations emerges from our analysis of the dependence of τ_1 on N.

APPENDIX B: SCALING BEHAVIOR OF ROUSE—ZIMM MODEL

Because the DPD model exhibits behavior similar to the Rouse–Zimm model, the scaling behavior of Rouse–Zimm is examined to provide insight into the variation of the scaling exponents ν and α with chain length N. The chain-length-dependent values of these parameters can be obtained by evaluating the derivatives $d \ln R_g / d \ln N$ and $d \ln \tau_1 / d \ln N$ locally at discreet N values.

The mean-square radius of gyration is obtained by evaluating Eq. (A3) at $t = 0$,

$$R_g^2 = C(0) = \frac{1}{N} \sum_i \frac{\langle Q_i'(0)^2 \rangle}{a_i} = \frac{3kT}{H} \frac{1}{N} \frac{N^2 - 1}{6}, \tag{B1}$$

which utilizes the equilibrium result $\langle Q_i'(0)^2 \rangle = 3kT/H$, where H is the spring constant. We can determine the Rouse–Zimm scaling exponent for R_g from the derivative of Eq. (B1):

$$\nu_N = \frac{d \ln R_g}{d \ln N} = \frac{N^2}{N^2 - 1} - \frac{1}{2}. \tag{B2}$$

For relaxation-time scaling, we examine the longest relaxation time of the Zimm model:

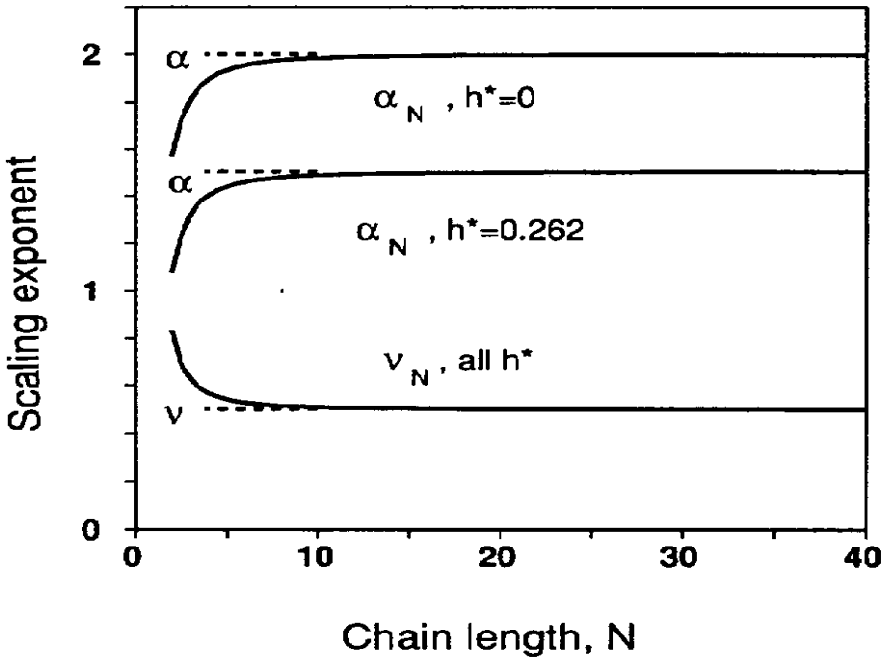

FIG. 6. Variation of scaling exponents with length of chain N, as predicted by the Rouse–Zimm theory. Local values for the scaling exponents ν and α are evaluated using Eqs. (B2) and (B4), respectively.

$$\tau_1 = \frac{\zeta}{2H\tilde{a}_1} \approx \frac{\zeta/2H}{4\sin^2(\pi/2N)} \frac{N^\sigma}{\beta}, \tag{B3}$$

where the Thurston approximation [see Eqs. (A6)–(A8)] has been employed to obtain the expression on the RHS. From Eq. (B3), we obtain

$$\alpha_N = \frac{d\ln\tau_1}{d\ln N} \approx \sigma + \frac{\pi}{N}\cot(\pi/2N). \tag{B4}$$

The local scaling exponents from the above analysis are plotted as a function of chain length N in Fig. 6. For $N > 10$, both ν_N and α_N closely approach their large-N limits, $\nu = \lim_{N\to\infty} \nu_N = 0.5$ and $\alpha = \lim_{N\to\infty} \alpha_N = 2 + \sigma$; thus we see that Rouse–Zimm chains reach the static and dynamic scaling regimes at surprisingly short chain lengths. The close similarities between the DPD chain and the Rouse–Zimm model suggest that DPD chains might also reach the scaling regime for $N > 10$. Applying this guideline, the scaling exponents reported in Table II for the DPD weak spring may not represent true large-N behavior because the simulations were done only for chains up to ten beads long. However, the DPD strong spring results were determined for chains up to 30 beads in length, which surely have reached true scaling behavior.

References

Adam, M. and M. Delsanti, "Dynamic properties of polymer solutions in good solvent by Rayleigh scattering experiments," Macromolecules **10**, 1229 (1977).

Bird, R. B., C. F. Curtiss, R. C. Armstrong, and O. Hassager, *Dynamics of Polymeric Liquids* (Wiley, New York, 1987), Vol. 2, pp. 151–179.

de Gennes, P. G., *Scaling Concepts in Polymer Physics* (Cornell University, Ithaca, 1979), p. 38; pp. 165–203.

Doi, M. and S. F. Edwards, *The Theory of Polymer Dynamics* (Clarendon, Oxford, 1986), pp. 91–139.

Fixman, M. and J. Kovac, "Dynamics of stiff polymer chains. II. Freely jointed chain," J. Chem. Phys. **61**, 4950–4954 (1974).

Hoogerbrugge, P. J. and J. M. V. A. Koelman, "Simulating microscopic phenomena with dissipative particle dynamics," Europhys. Lett. **19**, 155 (1992).

Koelman, J. M. V. A. and P. J. Hoogerbrugge, "Dynamics simulations of hard-sphere suspensions under steady shear," Europhys. Lett. **21**, 363 (1993).

Manke, C. W. and M. C. Williams, "Comparison of a new internal viscosity model with other constrained-connector theories of dilute polymer solution rheology," Rheol. Acta **32**, 418–421 (1993).

Pierleoni, C. and J.-P. Ryckaert, "Relaxation of a single chain molecule in good solvent conditions by molecular-dynamics simulations," Phys. Rev. Lett. **66**, 2992 (1991).

Pierleoni, C. and J.-P. Ryckaert, "Molecular dynamics investigations of dynamic scaling for dilute polymer solutions in good solvent conditions," J. Chem. Phys. **96**, 8539 (1992).

Thurston, G. B., "Exact and approximate eigenvalues and intrinsic functions for the Gaussian chain theory," Polymer **15**, 569–572 (1974).

Zylka, W. and H. C. Öttinger, "A comparison between simulations and various approximations for Hookean dumbbells with hydrodynamic interaction," J. Chem. Phys. **90**, 474–480 (1989).